Determination of ionization energies of small silicon clusters with vacuum-ultraviolet (VUV) radiation.

Oleg Kostko, Stephen R. Leone,[1] Michael A. Duncan[2] and Musahid Ahmed*

Chemical Sciences Division, Lawrence Berkeley National Laboratory, Berkeley, CA 94720, USA

[1]Department of Chemistry and Physics, University of California at Berkeley, Berkeley, CA 94720, USA

[2]Department of Chemistry, University of Georgia, Athens, GA 30602, USA

* Corresponding author: MS: 6R-2100, Lawrence Berkeley National Laboratory, 1 Cyclotron Road, Berkeley, CA-94720, USA. Phone: (510) 486-6355; fax: (510) 486-5311; e-mail: MAhmed@lbl.gov

Abstract

In this work we report on single photon vacuum ultraviolet photoionization of small silicon clusters (n=1-7) produced via laser ablation of Si. The adiabatic ionization energies (AIE) are extracted from experimental photoionization efficiency (PIE) curves with the help of Frank-Condon simulations, used to interpret the shape and onset of the PIE curves. The obtained AIEs are (all energies are in eV): Si (8.13±0.05), Si_2 (7.92±0.05), Si_3 (8.12±0.05), Si_4 (8.2±0.1), Si_5 (7.96±0.07), Si_6 (7.8±0.1), and Si_7 (7.8±0.1). Most of the experimental AIE values are in good agreement with density functional electronic structure calculations. To explain observed deviations between the experimental and theoretical AIEs for Si_4 and Si_6, a theoretical search of different isomers of these species is performed. Electronic structure calculations aid in the interpretation of the $a^2\Pi_u$ state of Si_2^+ dimer in the PIE spectrum. Time dependent density functional theory (TD-DFT) calculations are performed to reveal the energies of electronically excited states in the cations for a number of Si clusters.

Keywords: Laser ablation, molecular beams, synchrotron radiation, electronic structure theory

Introduction

Silicon cluster ions were observed in an electron impact ionization study by Honig as early as 1954.[1] With the advent of the microelectronics industry based around silicon, in the 80's, there was an explosion in the study of the electronic properties of silicon clusters and extrapolation of these properties to the bulk phase.[2] Recently there has been a resurgence of the study of small silicon clusters and doped silicon clusters, modeled as building blocks for smart materials and nanowires.[3] There is also interest in studying the fluxional and aromatic behavior of small silicon clusters.[4] However, one electronic property that could aid in these endeavors, the ionization energies (IE) of small silicon clusters, has not been determined experimentally with great precision. There has been controversy in the ionization energy of the dimer,[5,6] while for the higher Si_n clusters ranging from n=3-7, there are a few bracketing studies with an precision of only around 0.5 eV.[7] We have started a systematic investigation to address this fundamental property and in this work we report an experimental and theoretical study of the ionization energies of Si_n (n=1-7) using vacuum-ultraviolet single photon ionization.

Very early work reported electron impact ionization energies for Si clusters.[8] Subsequently, two groups reported ionization energies for Si clusters using photoionization. Fuke et al.[7] performed bracketing measurements for cluster sizes between n=2-200, while Trevor et al.[9] reported that $Si_{2\text{-}7,10}$ species have IEs greater than 7.87 eV and that the higher clusters have IEs below 7.87 eV. The IE of the dimer has been measured using two photon ionization by Winstead et al.[10] (7.9-8.08 eV) and Marijnissen and ter Meulen (7.9206 eV),[11] while Boo and Armentrout[12] estimated the dimer IE thermodynamically to be $\leq$ 8.04 eV. In light of these experimental results, Dixon et al.[6] commented on the role of excited electronic states in the photoionization of the silicon dimer. Very recently, Jaeger et al.[13] estimated the ionization energy of Si_7 to be between 6.77-7.58 eV from photodissociation studies of metal-silicon clusters. In contrast to these relatively few experimental determinations, there have been a number of

theoretical calculations of the IEs of Si clusters at various levels of theory, and while relative trends in decreasing IE with increasing cluster size tend to agree, the absolute IEs have varied considerably.[4,14-20]

At the chemical dynamics beamline, we have performed a number of photoionization studies on clusters generated by laser ablation coupled to supersonic molecular beams.[21-23] Tunable VUV generated at a synchrotron provides a convenient source for single photon ionization of these species. We applied the method to generate and study Si_n clusters up to n=7. Electronic structure calculations were performed to aid in the interpretation of the photoionization results. The extracted AIEs represent a significant improvement of the previous experimental values which were mostly from bracketing techniques with considerable uncertainties and in some cases fall completely outside our reported IE values. The experimental IE's measured in this work have error bars ranging from ±0.05 to 0.1 eV depending on cluster size and represents a more precise number. TD-DFT calculations of cluster excited states together with the analysis of the photoionization of different Si_4 and Si_6 isomers explain the shapes of the experimental PIE curves.

Experimental Section

The experiment is performed on a laser ablation apparatus coupled to a 3 m monochromator at the Chemical Dynamics Beamline (9.0.2) at the Advanced Light Source. The experimental apparatus used for the cluster production is the same as used recently for preparation of gas phase SiO_2 and carbon clusters.[21,22] It consists of a laser ablation molecular beam cluster source and a time-of-flight mass spectrometer. A rotating and translating 6.35 mm diameter silicon rod inside a Smalley-type cluster source[24] is ablated by focused radiation from the second harmonic (532 nm) of a 50 Hz pulsed Nd:YAG laser. The ablation laser energy employed in this study is about 0.62 mJ/pulse. A beam of pure argon is introduced through a pulsed valve located behind the rod for the cooling of the ablated material. The temperature of the clusters after travelling through a 25 mm long, 4 mm in diameter room temperature

nozzle is estimated to be about 300 K. It was observed that the PIE curve of C_3 obtained using the same setup shows a sharper onset than was observed previously,[23] demonstrating more efficient cooling and quenching of electronically and vibrationally excited states in this work. Ionized silicon clusters, produced directly in the ablation region, are deflected out of the molecular beam by an electrical field. Neutral Si clusters are skimmed and ionized by synchrotron VUV radiation inside the interaction region of a reflectron time-of-flight (TOF) mass spectrometer. Since the synchrotron light is quasi-continuous (500 MHz), a pulsed field directing the ionized clusters into the flight tube is used as a start pulse for the TOF measurement. This pulse is synchronized with the ablation laser and pulsed valve. After acceleration and passage through the flight tubes and reflectron, ions are detected by a microchannel plate detector. The time-dependent signal is amplified by a fast preamplifier, collected by a multichannel-scalar card and analyzed with a PC computer. Time-of-flight mass spectra are collected for photon energies in the range of 7.4 to 10.5 eV with a step size of 0.05 eV. Each mass spectrum was recorded for 2-4 thousand sweeps at a repetition rate of 50 Hz. The photoionization efficiency curves are obtained by integrating over the peaks in the mass spectrum at each photon energy. The spectra presented are the average of seven photon energy scans. A fitting procedure similar to that used by Nicolas et al.[23] for C_3 generated using similar techniques is applied to generate the error in the photoionization thresholds. In this procedure, the rising edge of the PIE curve from background is constrained by straight lines, and the intercept of these lines with the energy axis generates the error limit of the threshold measurement. The synchrotron VUV photon flux used for spectra normalization is measured by a Si photodiode. Argon or krypton gases (for the low photon energy region) are used in a gas filter to block the higher harmonics of the undulator synchrotron radiation. Absorption lines of argon are used for energy calibration of the PIE spectra.

Results and Discussion

A typical mass spectrum obtained at a photon energy of 9 eV is shown in Figure 1. Mass spectra obtained in this experiment are calibrated with the masses of rare gases such as krypton and xenon, which have rich isotope distributions. Peaks corresponding to the Si_n^+ species, where n=1-7, are observed in the spectrum. The isotope distribution of silicon clusters observed in the experiment corresponds to the expected one, and an example of Si_7 is shown in the inset of Figure 1. While the peaks corresponding to Si_2 to Si_7 have similar intensities, that of the silicon monomer is about six times greater. Attempts were made to change the experimental conditions such as the ablation laser intensity and the delays between the laser and cooling gas pulses and the mass spectrometer extraction pulse, to increase the intensity of larger clusters. Clusters above Si_7 were observed, however their intensities were insufficient to extract photoionization efficiency curves.

The mass spectrum shown in Figure 1 differs from several spectra published previously by other groups.[7,25-28] Heath et al.[25] and Bloomfield et al.[26] observed an increased intensity of peaks (magic numbers) for Si_6^+ and Si_{10}^+. The use of multiphoton ionization with an ArF excimer laser in their work caused fragmentation of large clusters, producing daughter ions in the 6-11 atom size range, where Si_6 and Si_{10} are of particular stability.[25] In our case, soft single photon ionization with energies just above the ionization threshold leads to a more even peak intensity distribution with a slight odd/even alternation, as shown in Figure 1. The prominent peak at m/z 40 corresponds to Ar, the backing gas used for cluster formation and arises from Rydberg state ionization.

Photoionization curves for the silicon clusters measured in the photon energy range from 7.4 to 9 eV are shown in Figure 2. Due to the low density of silicon clusters in the ionization region, the PIE curves are relatively noisy compared to other experiments performed with this apparatus. Whereas for some cluster sizes the appearance energies can be immediately found, for the rest, the energies of the onsets are not so obvious. To aid in the interpretation of the PIE spectra, DFT calculations of the adiabatic ionization energies were performed. Geometry optimizations were carried out using the B3LYP

hybrid functional with the 6-311+g(d) basis set using the Gaussian 03 program package[29] for both the neutral and cation ground states without symmetry constraints. The calculated ground state structures for the cluster cations, which do not significantly differ from those of the neutral species, are shown in Figure 2 and their coordinates are available in Supporting Information. The silicon cluster geometries obtained in this work are very similar to those obtained in numerous other theoretical investigations.[17,18,30-33] For the silicon dimer, the neutral ground state is a triplet and that of the cation is a quartet, while the trimer and larger clusters have neutral ground states that are singlets with doublet spins for the cations. The tetramer is the largest cluster having a two dimensional (2D) structure, whereas Si_5 and larger clusters have 3D structures.

AIEs were obtained from the differences in the zero-point corrected electronic energies for each neutral cluster and its corresponding cation. The vertical ionization energies (VIEs) were found by single-point energy calculations of the cations at the respective neutral ground-state geometries. The results of these calculations are shown in Table 1. The obtained IE of atomic silicon is in excellent agreement with the literature value of 8.15166±0.00003 eV.[34] The AIE values for the dimer and larger clusters exhibit an odd/even alternation, the odd sizes having larger AIEs, which has been observed in previous calculations.[16,18] The numerous calculations of silicon cluster IEs at different levels of theory exhibit large variations in the obtained values; these calculated IEs[14-16,18,32] are generally greater than those calculated in this work. An analysis of the AIE and VIE data shows that the difference between AIE and VIE is greatest for Si_4 and Si_6, revealing poor Franck-Condon factors (FCF) and significant geometry changes upon ionization. Moreover in our and previous calculations, the IE for Si_4 is significantly lower than the IE values for the adjacent trimer and pentamer.[16,18] In this work the difference between calculated AIE values of Si_3 and Si_4 is 0.2 eV, the Si_3 having the larger AIE (see Table 1). An examination of the experimental PIE curves reveals that in the case of Si_3 and Si_4 the onset of signals appear approximately at the same energy, in contrast to the calculated AIEs. Further analysis of the PIE curve onsets and the

positions of the AIEs shown in Figure 2 indicate that in some cases they roughly coincide while in other cases the correlation is not obvious.

For a more detailed analysis of the experimental data, the FCFs for these ionization transitions were found. The FCFs were calculated within the harmonic approximation, and hot band contributions were included. Using the FCFs and the vibrational frequencies obtained in calculations, we simulated photoelectron spectra, which were convoluted with a Gaussian function having 50 meV FWHM, corresponding to the energy profile of the synchrotron beam used in the experiment. Integration of the theoretical photoelectron spectrum, assuming constant photoionization cross-section and absence of dissociation channels, generates a PIE curve. This analysis was performed recently in the study of SiO_2.[22] The onset of the generated PIE curve (first 0.5 eV of the spectrum) was fitted to the experimental intensity and energy profile. The fitted curves as well as the positions of the 0-0 transition (corresponding to the AIE) obtained from the fit are shown in Figure 2, and these values are listed in Table 1. For most of the clusters, particularly the odd numbered ones, the calculated AIEs and the fit values lie close in energy (the difference is at most 40 meV for Si_3). On the other hand, for the even numbered Si_4 and Si_6 species, the difference exceeds 0.25 eV. The measured AIEs are shown in Figure 3 together with the values obtained from DFT calculations and the previous experimental data measured by Brown et al.,[34] Marijnissen et al.,[11] Fuke et al.[7,28] and Jaeger et al.[13] One immediately sees that while the AIE value found by Marijnissen et al. for the dimer coincides extremely well with our result, the AIEs obtained by Fuke et al. for Si_2 and Si_3 are more than 0.3 eV above the values found in this work. Their AIE values for Si_4, Si_5 and Si_6 correlate well with ours, whereas for Si_7 the bracketing value measured by Fuke et al. is within the error bars of the value measured in this work and the value obtained by Jaeger et al. from the analysis of the photodissociation of metal-silicon clusters lies 0.2 eV below our value. Thus we are demonstrating a significant improvement of the AIE values for Si clusters in comparison to the ionization energy range previously accessed with the bracketing method.

The differences between the AIE values obtained in the calculations and the experiments for Si_4 and Si_6 are not the only disagreement between the derived and experimental PIEs. For certain cluster sizes (Si_n, n=2, 3, 5, 7) at higher photon energies the experimental data deviates from the derived PIE. One possible explanation of the observed features could be dissociation of larger clusters leading to fragment daughter ions filling in this mass, however the high dissociation energies of Si_n in this size regime of about 3 eV[17] negates this hypothesis. On the other hand, these features appearing at higher photon energies resemble the structure that might result from the production of higher lying electronic states of the cations. To test this hypothesis we performed TD-DFT calculations of the excited electronic states for these cluster cations. We chose this approach since TD-DFT in the past have shown good agreement with experimental results[22,35] and the low cost and simplicity makes it a useful tool when combining experimental and theoretical studies. The vertical excitation energies, obtained at the TD-DFT (B3LYP/6-311+g(d)) level of theory are shown in Figure 2 by vertical sticks, and these are listed in Table 1. A good correlation between the VIE position of the first excited state and the step in the intensity of the experimental PIE curves and the fact that the VIEs of excited states of Si_4^+ and Si_6^+ are above 9 eV suggest that excited states of the cation are being accessed at higher photon energies.

For the silicon dimer the feature observed in Figure 2 above 8.3 eV is due to ionization of the $X^3\Sigma_g^-$ neutral state of Si_2 to form the $a^2\Pi_u$ excited state of Si_2^+. The latter state lies 0.44 eV above the $X^4\Sigma_g^-$ ground state of Si_2^+ at the B3LYP/6-311+g(d) level of theory (see Table 1). Franck-Condon factors for this transition were calculated in this work and the simulated PIE curve is shown in Figure 2. The excellent agreement between the calculation results and experimental data confirms our hypothesis about the origin of this observed feature.

The above mentioned disagreement of the experimental and calculated AIEs for Si_4 and Si_6 could be explained either by different spin multiplicities for the neutral and cation clusters and/or by the presence in the molecular beam of different cluster isomers. The most abundant Si_4 isomer appearing in

the theoretical literature has a rhombus shape with D_{2h} symmetry.[17,18,32,33,36,37] However, while the rhombus Si_4 is the ground state species, there are a number of different isomers close to this in energy.[30,31,38] One theoretical investigation using an empirical tight-binding method has reported that the most stable Si_4 isomer is a tetrahedron with T_d symmetry.[39]

We performed an extensive theoretical search for Si_4 and Si_4^+ isomers having different spin multiplicities. For neutral Si_4 we considered singlet and triplet spins, whereas for Si_4^+ the doublet and quartet states were considered. Five different isomer symmetries were investigated: D_{2h} (rhombus), D_{4h} (square), T_d (tetrahedral), C_{2v}, and $D_{\infty h}$ (linear), and the corresponding structures are shown in Figure 4 and the coordinates of the isomers are provided in Supporting Information. The relative energies and electronic states found for the isomers with the B3LYP functional and 6-311g basis set are shown in Table 2. For D_{4h} we did not find any stable isomer. In our isomer search we also observed that the most stable isomeric form of both the neutral and positively charged silicon tetramer is a rhombus with D_{2h} symmetry. But the adiabatic ionization energy, corresponding to a singlet to doublet ionization transition, is about 0.3 eV below that observed in our photoionization experiment. Ionization energies for different isomers having the same symmetry have AIE values that strongly differ from the experimental values and are listed in Table 2. After taking into consideration all the possible transitions listed in Table 2, it is found that there are three transitions that lie close to the experimental AIE value of 8.2±0.1 eV. These are the above mentioned $^2B_u \leftarrow {}^1A_g$ transition, a $^4\Sigma_g^- \leftarrow {}^3A''$ transition with higher AIE, and the $^2A \leftarrow {}^3A_u$ transition with even higher AIE. At the B3LYP/6-311g level, the AIE for the second transition ($^4\Sigma_g^- \leftarrow {}^3A''$) is 8.12 eV, and for the third one ($^2A \leftarrow {}^3A_u$) it is 8.33 eV, both of which are close to the experimental value. A qualitative analysis of the isomer geometries participating in the transitions reveals that the third transition ($^2A \leftarrow {}^3A_u$) is very improbable since this involves a significant geometry change (from the rhombus to the linear isomer). The second transition ($^4\Sigma_g^- \leftarrow {}^3A''$) is more probable since this involves a less significant geometry change upon ionization (C_{2v} isomer transforms into a linear one).

This is partially supported by the shape of the experimental PIE (Figure 2). A less steep slope of the experimental PIE comparing to the theoretical (obtained for D_{2h} symmetry) data suggests a different isomer and a more significant geometry change. Nevertheless, it should be noted that two theoretical and experimental investigations of small silicon clusters deposited into gas matrices using either Raman or infrared absorption spectroscopies[40,41] suggest that the rhombus (D_{2h}) cluster isomer is the dominant tetramer species, hence further computational effort is required to completely identify the structure of the ionized silicon tetramer.

Numerous theoretical investigations of Si_6 have considered the C_{2v} and D_{4h} symmetries for isomeric structures.[17,18,33,36,37] In some investigations, the D_{4h} isomer was found to be more stable for the neutral clusters,[33,37] however the majority of these studies claim C_{2v} as the most stable isomer. Kang et al. found that C_{2v} and D_{4h} isomers are essentially degenerate with an energy barrier between them around 10^{-4} eV and concluded that these two symmetries coexist in the ground state of the Si_6 cluster.[36] Liu et al. and Nigam et al. found that the edge-capped trigonal C_{2v} structure is nearly degenerate with the D_{4h} structure, with an energy difference of 0.03 eV, the former being the lowest isomer.[17,18] It was also found that the silicon hexamer exhibits fluxional behavior, sampling a symmetric D_{4h} structure separated by a very low energy barrier from a C_{2v} isomer.[4] The $^3T_{1g}$ state of Si_6 with O_h symmetry was found to be the most stable hexamer structure by Pacchioni and Koutecky.[31]

For Si_6 we considered three different isomers with C_s (edge-capped trigonal bipyramid, shown in Figure 2), D_{4h} (tetragonal bipyramid) and O_h (octahedron) symmetries.[30,31] In our geometry optimization search we were unable to find stable minima for D_{4h} or O_h geometries. For the neutral C_s isomer the singlet is found to be about 0.7 eV below the triplet state. For cationic Si_6 a C_{2v} symmetry was found, which is very close to the symmetry of the neutral C_s. Liu et al. have calculated the AIEs and VIEs for C_{2v} and D_{4h} isomers of Si_6 using DFT in the local density approximation (LDA) and the Perdew-Wang-Becke 88 (PWB) functional.[18] They found in both cases that the D_{4h} isomer has the larger AIE, differences of

0.19 eV (LDA) and 0.25 eV (PWB functional), compared to that for the C_{2v} isomer. These values are in good agreement with the difference of about 0.26 eV between the AIE for the C_{2v} isomer and the observed experimental onset in our work. Therefore we conclude that we may have a greater population of D_{4h} isomers in the experimental cluster beam. This is indirectly supported by previous experimental investigations. The D_{4h} isomer of Si_6 was also found in the investigations of Honea et al. and Li et al. where either Raman or IR absorption spectroscopy investigations were performed on Si clusters in a gas matrix.[40,41] Shvartsburg et al. in their theoretical work found that the global minimum structure for the neutral hexamer has D_{4h} symmetry, whereas for the Si_6^+ cluster cation the C_{2v} isomer was found to be more stable.[33] This edge-capped trigonal bipyramid isomer (with C_{2v} symmetry) was recently observed experimentally by Lyon et al. in an investigation of gas-phase silicon cluster cations using infrared multiple photon dissociation of their complexes tagged with Xe atoms.[41] This partly confirms our hypothesis that in the neutral cluster beam, the D_{4h} isomer is mostly populated (or the time average of fluxional Si_6 favors the D_{4h} structure[4]) and depending on the beam conditions this may fluctuate and transform into the C_{2v} isomer upon ionization While there is still ambiguity about the structure of the tetramer cluster observed in our experiment, for Si_6 both experiment and theory suggest that the favored structure isomer is the one with D_{4h} symmetry. Nevertheless further computational efforts, directly verifying the transition of D_{4h} to C_{2v} isomer and determination of FCFs for this transition would be helpful in untangling the complicated nature of silicon cluster isomers.

A complication in extracting ionization energies from threshold measurements could arise from excited electronic and vibrational states (hot bands) populating the neutral cluster beam leading to lower onsets than a true AIE. We saw evidence for this in the case of carbon clusters,[21,23] particularly from low lying excited electronic states in the smaller clusters (n=4-6). Neumark and co-workers[42] have extensively mapped out the energetics of these electronic states in the case of neutral silicon clusters using anion photo-detachment spectroscopy. We used these results to analyze the shapes of the Si

cluster PIE's; however, an examination of Figure 2 suggests that there is relatively minor signal below our measured AIE that is within the S/N of the experiment. This contrasts sharply with what was observed in the case of the carbon cluster work.[21,23] Better cooling with a longer ablation channel, sampling of a colder part of the pulsed beam, and possibly shorter lifetimes of the electronically excited states in the case of Si clusters could explain the difference in the shapes of the PIE's. The signature of vibrational hot bands in the case of neutral Si clusters could theoretically be extracted from calculated vibrational populations coupled with the calculated FCF's. However, the experimental PIE's measured in this work do not have sufficient sensitivity for us to extract a vibrational temperature since calculations of neutral cluster vibrational populations between 0-1500 K could all be fit with our experimental PIE's.

Conclusions

A joint experimental and theoretical study of VUV photoionization of small silicon clusters obtains experimental values for the IEs of Si_n (n=1-7). The IEs are extracted from experimental PIE curves and compared to the results of DFT electronic structure calculations. For interpretation of the shapes of the PIE curves, Franck-Condon factor simulations were undertaken. With the aid of TD-DFT calculations, it is found that the additional features at higher photon energy in experimental PIE curves are due to the production of electronically excited states of the cations. Numerous cluster isomers were investigated via density functional theory to resolve the ambiguity in the structures of the tetramer and hexamer; the latter was found most probably to have D_{4h} symmetry.

Acknowledgements:

This work was supported by the Director, Office of Energy Research, Office of Basic Energy Sciences, and Chemical Sciences Division of the U.S. Department of Energy under contract No. DE-AC02-05CH11231. O.K. acknowledges Jia Zhou for numerous helpful discussions. M.A.D. acknowledges support from the Air Force Office of Scientific Research.

Supplementary Information:

Atomic coordinates and bond lengths for silicon clusters shown in Figure 2 and tetramer silicon isomers shown in Figure 4 in neutral and cationic states**.**

References:

(1) Honig, R. E. *J. Chem. Phys.* **1954**, *22*, 1610.

(2) Baletto, F.; Ferrando, R. *Rev. Modern Phys.* **2005**, *77*, 371.

(3) Ferraro, M. B. *J. Comput. Meth. Sci. Eng.* **2007**, *7*, 195.

(4) Zdetsis, A. D. *J. Chem. Phys.* **2007**, *127*, 10.

(5) Winstead, C. B.; Paukstis, S. J.; Gole, J. L. *Chem. Phys. Lett.* **1995**, *237*, 81.

(6) Dixon, D. A.; Feller, D.; Peterson, K. A.; Gole, J. L. *J. Phys. Chem. A* **2000**, *104*, 2326.

(7) Fuke, K.; Tsukamoto, K.; Misaizu, F.; Sanekata, M. *J. Chem. Phys.* **1993**, *99*, 7807.

(8) Drowart, J.; Demaria, G.; Inghram, M. G. *J. Chem. Phys.* **1958**, *29*, 1015.

(9) Trevor, D. J.; Cox, D. M.; Reichmann, K. C.; Brickman, R. O.; Kaldor, A. *J. Phys. Chem.* **1987**, *91*, 2598.

(10) Winstead, C. B.; Paukstis, S. J.; Gole, J. L. *J. Mol. Spectrosc.* **1995**, *173*, 311.

(11) Marijnissen, A.; terMeulen, J. J. *Chem. Phys. Lett.* **1996**, *263*, 803.

(12) Boo, B. H.; Armentrout, P. B. *J. Am. Chem. Soc.* **1987**, *109*, 3549.

(13) Jaeger, J. B.; Jaeger, T. D.; Duncan, M. A. *J. Phys. Chem. A* **2006**, *110*, 9310.

(14) Vonniessen, W.; Zakrzewski, V. G. *J. Chem. Phys.* **1993**, *98*, 1271.

(15) Zhao, J. J.; Chen, X. S.; Sun, Q.; Liu, F. Q.; Wang, G. H. *Phys. Lett. A* **1995**, *198*, 243.

(16) Wei, S. Q.; Barnett, R. N.; Landman, U. *Phys. Rev. B* **1997**, *55*, 7935.

(17) Nigam, S.; Majumder, C.; Kulshreshtha, S. K. *J. Chem. Phys.* **2004**, *121*, 7756.

(18) Liu, B.; Lu, Z. Y.; Pan, B. C.; Wang, C. Z.; Ho, K. M.; Shvartsburg, A. A.; Jarrold, M. F. *J. Chem. Phys.* **1998**, *109*, 9401.

(19) Jo, C.; Lee, K. *Phys. Lett. A* **1999**, *263*, 376.

(20) Ishii, S.; Ohno, K.; Kumar, V.; Kawazoe, Y. *Phys. Rev. B* **2003**, *68*, 5.

(21) Belau, L.; Wheeler, S. E.; Ticknor, B. W.; Ahmed, M.; Leone, S. R.; Allen, W. D.; Schaefer, H. F.; Duncan, M. A. *J. Am. Chem. Soc.* **2007**, *129*, 10229.

(22) Kostko, O.; Ahmed, M.; Metz, R. B. *J. Phys. Chem. A* **2009**, *113*, 1225.

(23) Nicolas, C.; Shu, J. N.; Peterka, D. S.; Hochlaf, M.; Poisson, L.; Leone, S. R.; Ahmed, M. *J. Am. Chem. Soc.* **2006**, *128*, 220.

(24) Smalley, R. E. *Laser Chem.* **1983**, *2*, 167.

(25) Heath, J. R.; Liu, Y.; Obrien, S. C.; Zhang, Q. L.; Curl, R. F.; Tittel, F. K.; Smalley, R. E. *J. Chem. Phys.* **1985**, *83*, 5520.

(26) Bloomfield, L. A.; Freeman, R. R.; Brown, W. L. *Phys. Rev. Lett.* **1985**, *54*, 2246.

(27) Brown, W. L.; Freeman, R. R.; Raghavachari, K.; Schluter, M. *Science* **1987**, *235*, 860.

(28) Fuke, K.; Tsukamoto, K.; Misaizu, F. *Z. Phys. D: At., Mol. Clusters* **1993**, *26*, S204.

(29) Frisch, M. J. T., G. W.; Schlegel, H. B.; Scuseria, G. E.; Robb, M. A.; Cheeseman, J. R.; Montgomery, J. A., Jr.; Vreven, T.; Kudin, K. N.; Burant, J. C.; Millam, J. M.; Iyengar, S. S.; Tomasi, J.; Barone, V.; Mennucci, B.; Cossi, M.; Scalmani, G.; Rega, N.; Petersson, G. A.; Nakatsuji, H.; Hada, M.; Ehara, M.; Toyota, K.; Fukuda, R.; Hasegawa, J.; Ishida, M.; Nakajima, T.; Honda, Y.; Kitao, O.; Nakai, H.; Klene, M.; Li, X.; Knox, J. E.; Hratchian, H. P.; Cross, J. B.; Bakken, V.; Adamo, C.; Jaramillo, J.; Gomperts, R.; Stratmann, R. E.; Yazyev, O.; Austin, A. J.; Cammi, R.; Pomelli, C.; Ochterski, J. W.; Ayala, P. Y.; Morokuma, K.; Voth, G. A.; Salvador, P.; Dannenberg, J. J.; Zakrzewski, V. G.; Dapprich, S.; Daniels, A. D.; Strain, M. C.; Farkas, O.; Malick, D. K.; Rabuck, A. D.; Raghavachari, K.; Foresman, J. B.; Ortiz, J. V.; Cui, Q.; Baboul, A. G.; Clifford, S.; Cioslowski, J.; Stefanov, B. B.; Liu, G.; Liashenko, A.; Piskorz, P.; Komaromi, I.; Martin, R. L.; Fox, D. J.; Keith, T.; Al-Laham, M. A.; Peng, C. Y.; Nanayakkara, A.; Challacombe, M.; Gill, P. M. W.; Johnson, B.; Chen, W.; Wong, M. W.; Gonzalez, C.; Pople, J. A. Gaussian 03; Gaussian Inc.: Pittsburgh, Pa, 2004.

(30) Fournier, R.; Sinnott, S. B.; Depristo, A. E. *J. Chem. Phys.* **1992**, *97*, 4149.

(31) Pacchioni, G.; Koutecky, J. *J. Chem. Phys.* **1986**, *84*, 3301.

(32) Raghavachari, K.; Logovinsky, V. *Phys. Rev. Lett.* **1985**, *55*, 2853.

(33) Shvartsburg, A. A.; Liu, B.; Jarrold, M. F.; Ho, K. M. *J. Chem. Phys.* **2000**, *112*, 4517.

(34) Brown, C. M.; Tilford, S. G.; Tousey, R.; Ginter, M. L. *J.Opt. Soc. Am.* **1974**, *64*, 1665.

(35) Stringer, K. L.; Citir, M.; Metz, R. B. *J. Phys. Chem. A* **2004**, *108*, 6996.

(36) Kang, D. D.; Hou, Y.; Dai, J. Y.; Yuan, J. M. *Phys. Rev. A* **2009**, *79*, 063202.

(37) Li, B. X.; Cao, P. L. *Phys. Rev. B* **2000**, *62*, 15788.

(38) Raghavachari, K. *J. Chem. Phys.* **1986**, *84*, 5672.

(39) Katircioglu, S.; Erkoc, S. *Chem. Phys. Lett.* **1991**, *184*, 118.

(40) Honea, E. C.; Ogura, A.; Murray, C. A.; Raghavachari, K.; Sprenger, W. O.; Jarrold, M. F.; Brown, W. L. *Nature* **1993**, *366*, 42.

(41) Li, S.; Vanzee, R. J.; Weltner, W.; Raghavachari, K. *Chem. Phys. Lett.* **1995**, *243*, 275.

Tables

Table 1. Calculated AIE and VIE values for Si_n clusters, obtained at B3LYP/6-311+g(d) level of theory for geometries shown in Figure 2, and values of experimental AIEs obtained from fits of calculated PIEs to experimental data. Additionally the energies corresponding to the VIEs (for all species but Si_2) of the first excited state are listed. For Si_2 this value corresponds to the AIE. Previous experimentally measured values of ionization energies are shown for comparison. All energies are in eV.

n	AIE	VIE	Experimental AIE	1st excited state	Previous experimental IE values
1	8.11	8.11	8.13±0.05		8.15166±0.00003[a]
2	7.92	7.92	7.92±0.05	8.36	>8.49[b], >7.87[c], 7.9-8.08[d], ≤8.04[e], 7.9206[f]
3	8.08	8.20	8.12±0.05	8.99	>8.49[b], >7.87[c]
4	7.88	8.11	8.2±0.1	9.21	7.97-8.49[b], >7.87[c]
5	7.96	8.13	7.96±0.07	8.64	7.97-8.49[b], >7.87[c]
6	7.56	7.95	7.8±0.1	9.05	~7.90[b], >7.87[c]
7	7.73	7.97	7.8±0.1	8.96	~7.90[b], >7.87[c], 6.77-7.58[g]

a[34]; b[7]; c[9]; d[10]; e[12]; f[11]; g[13]

Table 2. Relative electronic energies and states for Si_4 isomers with the different symmetries shown in Figure 3. All energies are in eV.

Isomer	neutral		cation		Ionization energies		
symmetry	singlet	triplet	doublet	quadruplet	doublet←singlet	doublet←triplet	quadruplet←triplet
D_{2h}	^1A_g 0.00	^3A_u 0.83	^2B_u 0.00	–	7.88	7.06	–
T_d	^1A 2.44	^3A 0.86	–	–	–	–	–
C_{2v}	–	$^3A''$ 1.41	$^2A'$ 0.64	$^4A''$ 1.23	–	7.11	7.70
$D_{\infty h}$	^1A 2.23	$^3\Sigma_g^-$ 1.72	^2A 1.27	$^4\Sigma_g^-$ 1.64	6.93	7.43	7.80

Figure Captions:

Figure 1. The mass spectrum obtained at 9 eV photon energy. The isotopic distribution for Si_7 is shown in the inset by the black solid line. The calculated isotopic distribution is shown by light magenta columns for comparison.

Figure 2. Photoionization efficiency curves for Si_n clusters, n=1-7. Circles and black lines correspond to the averaged experimental data. The standard deviation of seven experimental scans is shown as a wide grey line. The solid red lines represent derived PIEs from calculations, fitted to the experimental data. For the dimer an additional line starting at about 8.3 eV corresponds to the derived PIE for the $a^2\Pi_u \leftarrow X^3\Sigma_g^-$ ionization transition for silicon dimer. The positions of the calculated adiabatic ionization energies are shown by inverted triangles; the vertical ionization energy is represented by diamonds. The positions of the AIE values, obtained from fits of the derived PIEs to experimental data are shown by open circles. Calculated excited states of silicon cluster cations are shown by red vertical sticks. Structures, corresponding to the lowest isomers of Si_n cluster cations found in this work, are shown to the left and right of the PIE curves.

Figure 3. Experimental and calculated ionization energies for Si_n clusters. Open black circles represent experimental values for the AIEs. Red filled dots correspond to calculated AIEs at the B3LYP/6-311+g(d) level. For Si_4, open squares represent the AIEs of different cluster isomers found at the B3LYP/6-311g level. The plausible values of the AIEs for Si_4 and Si_6 are shown by gray symbols. Open triangles, marked LDA and PWB, correspond to two plausible AIEs for D_{4h} isomer of Si_6 at different levels of theory (see text for additional details). The experimental IEs obtained by Fuke et al.[7,28] by a bracketing method are shown by blue lines. The IE value found by Jaeger et al.[13] for Si_7 is shown by a green line. The experimental IEs found by Brown et al.[34] for atomic Si and by Marijnissen et al.[11] for Si_2 are shown by open blue diamonds.

Figure 4. The isomers of the Si_4 cluster considered in this investigation.

Figures

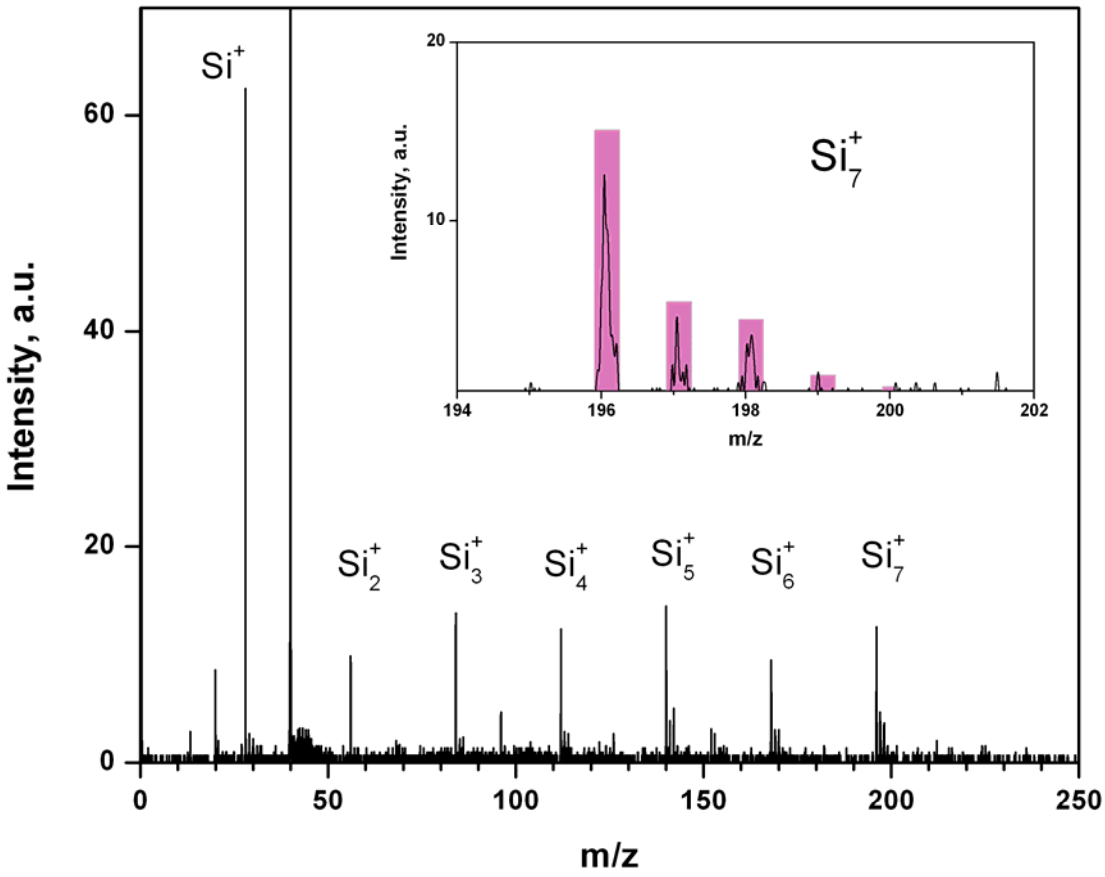

Figure 1.

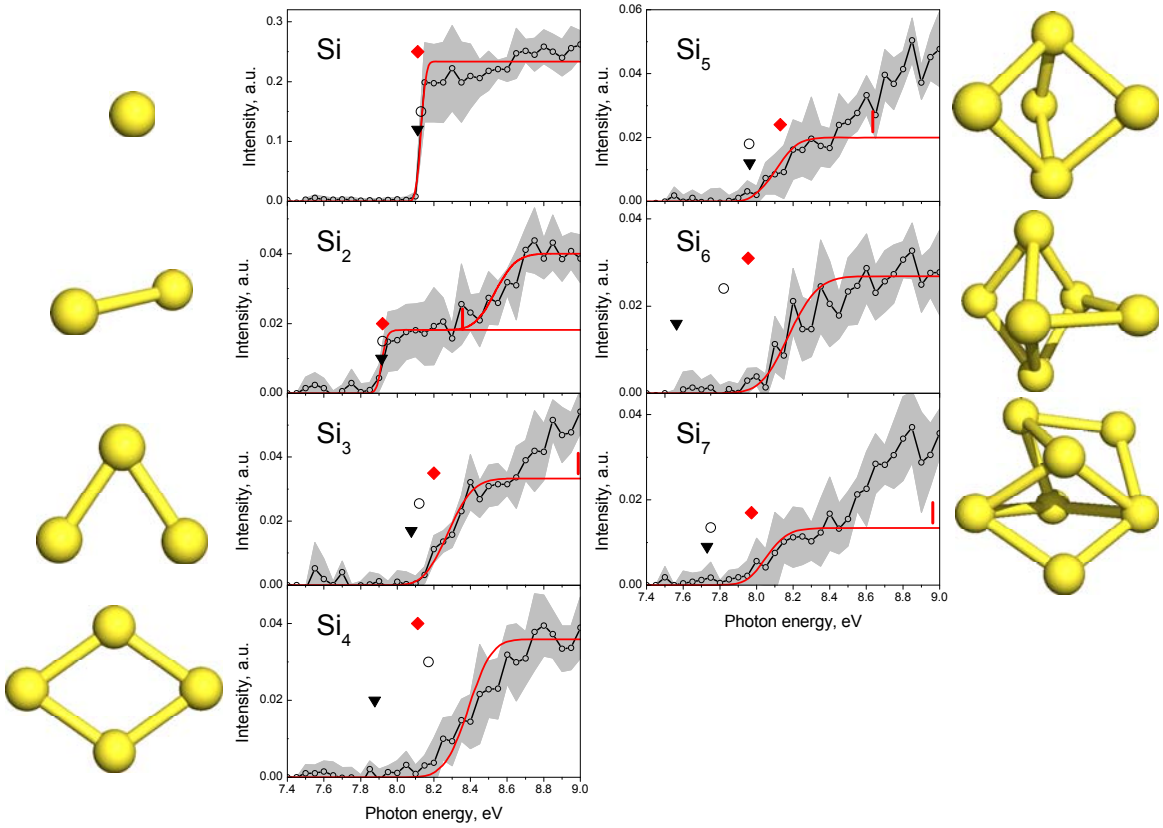

Figure 2.

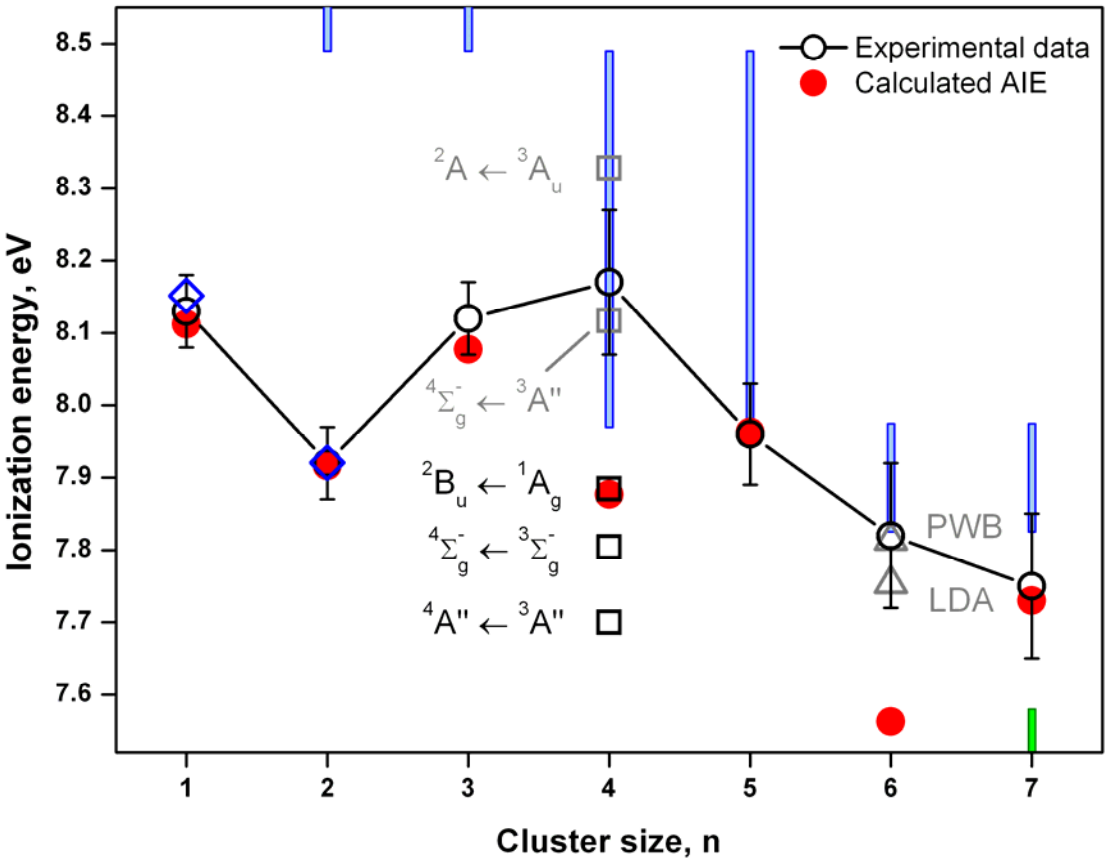
Ionization energy, eV
8.5
8.4
8.3
8.2
8.1
8.0
7.9
7.8
7.7
7.6
1
2
3
4
5
6
7
Cluster size, n
Experimental data
Calculated AIE
$^2A \leftarrow {}^3A_u$
$^4\Sigma_g^- \leftarrow {}^3A''$
$^2B_u \leftarrow {}^1A_g$
$^4\Sigma_g^- \leftarrow {}^3\Sigma_g^-$
$^4A'' \leftarrow {}^3A''$
PWB
LDA

Figure 3.

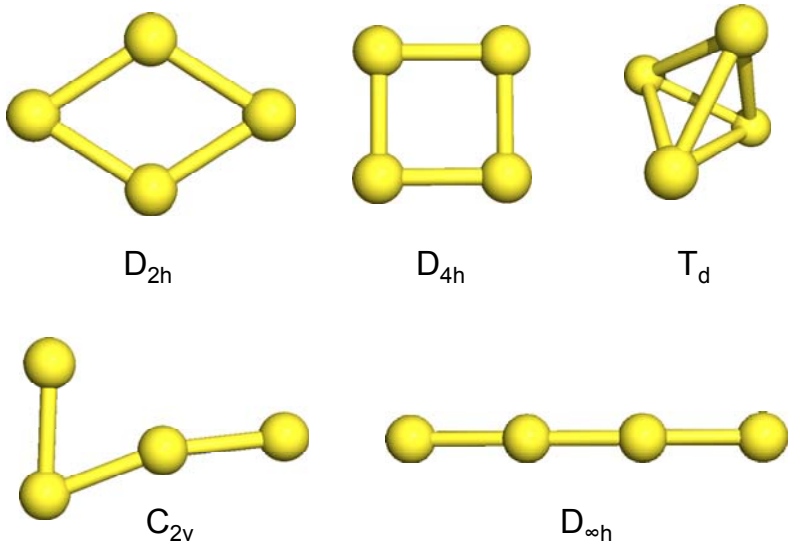

Figure 4.

Graphic for TOC